Small-Angle X-ray Scattering Studies of Liquid Crystalline 1-Alkyl-3-methylimidazolium Salts

A. E. Bradley,[†] C. Hardacre,*[,†,‡] J. D. Holbrey,[‡,§] S. Johnston,[‡] S. E. J. McMath,[†] and M. Nieuwenhuyzen[†]

The School of Chemistry and The QUILL Centre, The Queen's University of Belfast, Belfast BT9 5AG, Northern Ireland, United Kingdom

Received June 5, 2001. Revised Manuscript Received October 31, 2001

A series of long-chain 1-alkyl-3-methylimidazolium salts ([C_n−mim]X, n = 12−18) containing the anions, chloride, bromide, trifluoromethanesulfonate (OTf), and bis(trifluoromethanesulfonyl)imide (TFI), have been synthesized and characterized. The salts have amphiphilic characteristics, and the thermotropic phase behavior of these salts and the analogous tetrafluoroborate salt has been investigated by variable temperature small-angle X-ray scattering, polarizing optical microscopy, and differential scanning calorimetry. The salts form lamellar, sheetlike arrays in the crystalline phase and an enantiomeric smectic liquid crystalline phase at higher temperatures, except for the salts containing the bis(trifluoromethanesulfonyl)imide anion which melt directly to form isotropic liquids. The nature of the anion influences the size of the interlayer spacing in both the crystal and in the mesophase. The interlayer spacing in the mesophase is largest for the anions with the greatest ability to form a three-dimensional hydrogen-bonding lattice, following the order $[TFI]^- < [OTf]^- < [BF_4]^- < Br^- < Cl^-$.

Introduction

1-Alkyl-3-methylimidazolium salts are examples of room-temperature ionic liquids, i.e., liquids that are exclusively comprised of ions, which have a unique set of properties effectively including zero vapor pressure. These properties have led to the extension of ionic liquids as environmentally benign solvents for applications in "green chemistry".[1−3] Furthermore, there is considerable interest in the structural features of ionic liquid crystals,[4] for example, as oriented solvents which can impart selectivity in reactions by ordering reactants,[5] as templates for the synthesis of mesoporous and zeolitic materials,[6,7] and in the formation of ordered thin films.[8,9] The low melting points of the ionic liquids, which in some cases are as low as −90 °C,[10] are largely a function of packing frustration in the solid (which is dominated by the low-symmetry organic cations).[11] This reduces the lattice energy and inhibits crystallization. By employment of the same design rationale, mesogenic 1-alkyl-3-methylimidazolium salts with low melting points, compared with traditional ionic liquid crystalline alkylammonium and *N*-alkylpyridinium salts, may be prepared.

Examples of liquid crystalline 1-alkyl-3-methylimidazolium salts containing chloride,[12] hexafluorophosphate,[13,14] tetrafluoroborate,[15] and tetrachlorometalate (M = Co,[12] Ni,[12] Pd[16]) anions have been reported. Related 1,3-dialkylimidazolium and benzimidazolium salts have also been reported.[17] The mesomorphic behavior of the ionic liquid crystals obtained resemble those of the well-known cationic surfactants, *N*-alkylammonium salts, and aromatic heterocyclic systems, which form lamellar phases with a smectic bilayer structure.[18] To date, there have been no systematic studies of the influence of the anion type on the appearance and structure of the liquid crystalline phase

* To whom correspondence should be addressed. E-mail: c.hardacre@qub.ac.uk. Tel: +44 28 9027 4592. Fax: +44 28 9038 2117.
† The School of Chemistry.
‡ The QUILL Centre.
§ Current address: Center for Green Manufacturing, Chemistry Department, University of Alabama, Tuscaloosa, AL 35487.

(1) Holbrey, J. D.; Seddon, K. R. *Clean Prod. Proc.* **1999**, *1*, 233.
(2) Welton, T. *Chem Rev.* **1999**, *99*, 2071.
(3) Keim, W.; Wasserscheid, P. *Angew. Chem., Int. Ed.* **2000**, *39*, 3772.
(4) Abdallah, D. J.; Robertson, A.; Hsu, H.-F.; Weiss, R. G. *J. Am. Chem. Soc.* **2000**, *122*, 3053.
(5) Weiss, R. G. *Tetrahedron* **1988**, *44*, 3413.
(6) Jervis, H.; Raimondi, M. E.; Raja, R.; Maschmeyer, T.; Seddon, J. M.; Bruce, D. W. *J. Chem. Soc., Chem. Commun.* **1999**, 2031.
(7) Bradley, A. E. The Synthesis of Mesoporous Materials Using Novel Templates. Ph.D. Thesis, The Queen's University of Belfast, School of Chemistry, Northern Ireland, U.K., 1999.
(8) Yollner, K.; Popovitz-Biro, R.; Lahau, M.; Milstein, D. *Science* **1997**, *728*, 2110.
(9) Carmichael, A. J.; Hardacre, C.; Holbrey, J. D.; Nieuwenhuyzen, M.; Seddon, K. R. *Mol. Phys.* **2001**, *99*, 795.
(10) Larsen, A. S.; Holbrey, J. D.; Tham, F. S.; Reed, C. A. *J. Am. Chem. Soc.* **2000**, *122*, 7264.
(11) Wilkes, J. S.; Levisky, J. A.; Wilson, R. A.; Hussey, C. L. *Inorg. Chem.* **1982**, *21*, 1263.
(12) Bowlas, C. J.; Bruce, D. W.; Seddon, K. R. *J. Chem. Soc., Chem. Commun.* **1996**, 1625.
(13) Gordon, C. M.; Holbrey, J. D.; Kennedy, A.; Seddon, K. R. *J. Mater. Chem.* **1998**, *8*, 2627.
(14) Gordon, C. M.; Kennedy, A. R.; Triolo, A. Personal communication.
(15) Holbrey, J. D.; Seddon, K. R. *J. Chem. Soc., Dalton Trans.* **1999**, 2133.
(16) Hardacre, C.; Holbrey, J. D.; McCormac, P. B.; McMath, S. E. J.; Nieuwenhuyzen, M.; Seddon, K. R. *J. Mater. Chem.* **2001**, *11*, 346.
(17) Lee, K. M.; Lee, C. K.; Lin, I. J. B. *J. Chem. Soc., Chem. Commun.* **1997**, 899.
(18) Blackmore, E. S.; Tiddy, G. J. T. *J. Chem. Soc., Faraday Trans. 2* **1988**, *84*, 1115.

10.1021/cm010542v CCC: $22.00
Published on Web 01/16/2002

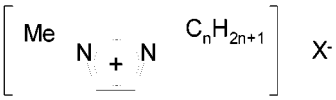

Figure 1. General structure of the salts studied, [C_n−mim]X (n = 12−20), based on the 1-alkyl-3-methylimidazolium cation.

of 1-alkyl-3-methylimidazolium salts. Abdallah et al.[4] have shown that in the neat phases of alkylphosphonium ionic liquid crystals, the nature of the anion plays a central role in the overall structure of the mesophase.

To understand the observations made from differential scanning calorimetry (DSC) and polarizing optical microscopy (POM) of mesomorphism for the 1-alkyl-3-methylimidazolium salts,[12−16] small-angle X-ray scattering (SAXS) measurements were performed. Here, we describe the synthesis and properties of the 1-alkyl-3-methylimidazolium salts [C_n−mim]X, n = 12−18, X = Cl^-, trifluoromethanesulfonate (triflate, OTf), and bis(trifluoromethanesulfonyl)imide (bis(trifyl)imide, TFI), and [C_n−mim]Br, n = 12−16, 20, as shown in Figure 1, and compare the SAXS of these salts with the previously reported tetrafluoroborate salts (n = 12−18).[15]

Experimental Section

All reagents and solvents (Aldrich) were used as received except for 1-methylimidazole which was distilled from calcium hydride prior to use. ^{1}H and ^{13}C NMR spectra were recorded in $CDCl_3$ or CD_3CN solution using a Bruker WM500 spectrometer at ambient temperature relative to tetramethylsilane, which was added as an internal standard. IR spectra were recorded using a Nicolet Impact 400D FTIR spectrometer in diffuse reflectance mode. Microanalyses were carried out by Analytical Services and Environmental Projects (The Queen's University of Belfast).

Examination of the Phases. Optical observations were made by heated-stage POM by using an Olympus BX50 microscope equipped with a Linkam TH600 hot stage and TP92 temperature controller. The phase transition temperatures were determined by DSC measurements carried out in a Perkin-Elmer Pyris 1 DSC equipped with a liquid nitrogen cryostatic cooler. Transition temperatures were determined under an inert nitrogen atmosphere by initially heating the sample from room temperature at a rate of 10 °C min^{-1} to beyond the clearing point, followed by three cooling−heating cycles at 10 °C min^{-1}. The transition temperatures and enthalpies of the transitions on the second and subsequent cycles were repeatable and reproducible.

Variable temperature SAXS experiments were carried out at the SRS, Daresbury, U.K., on beamline 8.2. Data were obtained from the salts in sealed 1 mm glass Lindemann by using a monochromated (1.54 Å) X-ray beam. Samples were transferred to the Lindemann tubes as molten liquids. A multiwire quadrant detector was used with a camera length of 0.95 m and an effective range of 8−190 Å. Heating was achieved by using a Linkam hot stage. The detector was calibrated with silver behenate.[19] The samples were heated and cooled at 6 °C min^{-1}, and data were collected in 12 s frames. Data reduction and analysis, correction for background scattering, and transmission and detector response were carried out by using XOTOKO.[20] In all cases, the samples were stationary and hence little can be inferred from the relative intensities of the peaks due to the possibility of preferential alignment.

Synthesis of the Salts. 1-Alkyl-3-methylimidazolium chloride salts (n = 12−18) were prepared in good yields (>90%, based on 1-methylimidazole) by the alkylation of 1-methylimidazole with the corresponding 1-chloroalkanes under solvent-free conditions at 80−120 °C in an inert atmosphere. The salts were obtained as hygroscopic solids, which were purified by recrystallization from 1,1,1-trichloroethane, isolated by filtration under nitrogen, dried in vacuo, and stored under nitrogen in a drybox. The bromide salts (n = 12−16, 20) were prepared by using an analogous procedure from the corresponding bromoalkanes and 1-methylimidazole.

[OTf]$^-$ and [TFI]$^-$ salts (n = 12−18) were prepared from the corresponding chloride salts by metathesis in water with sodium triflate and lithium bis(trifyl)imide, respectively, by using the procedure described by Bonhôte et al. for 1-ethyl-3-methylimidazolium bis(trifyl)imide.[21] The synthesis and characterization of the tetrafluoroborate salts has been reported previously.[15] Specific examples to illustrate the preparation of the salts are described below.

The chloride and bromide salts were obtained as waxy, hygroscopic solids. Diffuse reflectance IR spectroscopy on the halide salts shows an O−H stretching band in the region of 3500 cm^{-1} which is indicative of the presence of water in the samples. Elemental analysis and NMR spectroscopy indicated that the salts contained 1 mole of water. Rigorous exclusion of water during synthesis and workup stages enables the preparation of anhydrous salts; however, the salts readily absorb atmospheric moisture to form the stable monohydrates, which could be stored in air. It was not possible to remove all traces of water from the halide salts unless Schlenk techniques with rigorously dried materials and reagents were used. The SAXS data were obtained for the monohydrates.

The triflate and bis(trifyl)imide salts were isolated as colorless, anhydrous, low melting solids, which could be stored indefinitely in air.

The IR spectra in all cases are similar, except for an increase in aliphatic C−H stretch and bend intensities with n, and show characteristic stretching bands for the dialkylimidazolium cation.

1-Dodecyl-3-methylimidazolium Chloride, [C_{12}−mim]Cl. 1-Methylimidazole (40 cm^3, 0.5 mol) was placed in a 250 cm^3 three-necked round-bottomed flask, with a magnetic stirrer, in a nitrogen atmosphere. 1-Chlorododecane (121.1 cm^3, 0.515 mol) was added. The biphasic reaction mixture was heated with efficient stirring under reflux at 100−120° C for 48 h under dry nitrogen to give a viscous monophasic, pale yellow product. When the product was cooled to room temperature, the salt solidified and was recrystallized with 1,1,1-trichloroethane as colorless waxy crystals. The crystalline product was collected by filtration under nitrogen, dried in vacuo, and stored in a drybox (yield 116 g, 90%). ^{1}H NMR (500 MHz, $CDCl_3$): δ/ppm 0.87 (3H, t, J = 6.95 Hz, $-N(CH_2)_{11}CH_3$), 1.20−1.31(18H, m, $-NCH_2CH_2(CH_2)_9CH_3$), 1.89(2H, m, $-NCH_2CH_2(CH_2)_9CH_3$), 4.13 (3H, s, $-NCH_3$), 4.31 (2H, t, J = 7.47 Hz, NCH_2), 7.27 (1H, s, H(5)), 7.37 (1H, s, H(4)), 10.89 (1H, s, H(2)). ^{13}C NMR (75 MHz, $CDCl_3$): δ/ppm 14.08, 22.64, 26.24, 28.95, 29.31, 29.44, 29.54, 30.28, 31.86, 36.63, 50.19, 121.30, 122.95, 138.84. ν_{max}/cm^{-1} (KBr) 3481 (O−H), 3089, 3064 (s, aromatic C−H stretch), 2921, 2853 (s, aliphatic C−H stretch), 1635 (m), 1573, 1470 (s, symmetric ring stretch), 1446, 1389, 1356, 1290 (w), 1173 (s), 1091 (m), 886, 805, 754, 738 (m), 622 (s).

1-Dodecyl-3-methylimidazolium Triflate, [C_{12}−mim][OTf]. Sodium triflate (3.8 g, 0.022 mol) was added to a stirred solution of 1-dodecyl-3-methylimidazolium chloride (6.30 g, 0.022 mol) in H_2O (200 cm^3) at 70 °C. The solution was cooled to room temperature and formed a biphasic mixture. The upper, aqueous phase was decanted. The ionic liquid was dissolved in dichloromethane (50 cm^3) and washed with water (2 × 100 cm^3). The organic phase was then dried over $MgSO_4$, and the solvent was removed under reduced pressure and finally in vacuo at 55 °C to yield a colorless liquid. When the liquid was cooled to 4 °C, the salt crystallized as a white solid (yield 8.0 g, 91%). ^{1}H NMR (500 MHz, $CDCl_3$): δ/ppm 0.81 (3H, t, J = 6.60 Hz, $-N(CH_2)_{11}CH_3$), 1.18−1.25 (18H, m,

(19) Huang, T. C.; Toraya, H.; Blanton, T. N.; Wu, Y. *J. Appl. Crystallogr.* **1993**, *26*, 180.

(20) Boulin, C.; Kempf, R.; Koch, M. H. J.; McLaughlin, S. M. *Nucl. Instrum. Methods* **1996**, *A249*, 339.

(21) Bonhôte, P.; Dias, A. P.; Papageorgiou, N.; Kalyanasundaram, K.; Grätzel, M. *Inorg. Chem.* **1996**, *35*, 1168.

Table 1. Transition Temperatures and Enthalpies from DSC Thermograms for the Salts, [C_n−mim]X (for X = Cl^-, Br^-); Data from the First Heating Cycle Are for the Hydrated Salts, [C_n−mim]X·H_2O

			first heating		second heating	
n	anion, X^-	transition	*T*, °C	Δ*H*, kJ mol^{-1}	*T*, °C	Δ*H*, kJ mol^{-1}
12	[TFI]	cryst−iso	16.6	37.2	16.7	37.4
14		cryst−iso	34.7	38.7	34.3	41.4
16		cryst−iso	43.1	44.4	42.1	46.7
18		cryst−iso	44.8	51.3	44.8	50.0
12	[OTf]	cryst−iso	38.9	21.2	39.7	23.0
14		cryst−iso	54.0	32.1	53.6	33.0
16		cryst−SmA_2	59.6	23.7	58.1	24.9
		SmA_2−iso	71.6	0.7	70.2	0.6
18		cryst−SmA_2	63.8	30.2	66.0	33.8
		SmA_2−iso	107.4	0.9	107.5	1.0
12	Br	cryst−SmA_2	33.3	26.6	−5.3	6.7
		SmA_2−iso	115.5	0.21	81.97	0.37
14		cryst−SmA_2	46.1	41.4	20.8	13.3
		SmA_2−iso	176.0	1.0	162.9	0.8
16		cryst−SmA_2	66.0	65.6	40.2	21.3
		SmA_2−iso	219.7	1.2	207.5	1.0
20		cryst−SmA_2	76.5	73.2	60.2	27.3
		SmA_2−iso	239.9	0.1	*a*	
12	Cl	cryst−SmA_2	44.5	35.2	−2.8	2.76
		SmA_2−iso	151.7	0.1	104.4	0.6
14		cryst−SmA_2	49.1	41.6	19.4	3.62
		SmA_2−iso	187.7	1.2	162.5	0.8
16		cryst−SmA_2	66.7	59.7	42.0	16.8
		SmA_2−iso	222.2	2.1	204.0	0.5
18		cryst−SmA_2	71.7	65.5	53.2	26.9
		SmA_2−iso	221.9	1.7	*a*	

[a] The liquid crystal to isotropic phase change was too weak and broad to be accurately identified on the second heating for these salts.

$-NCH_2CH_2(CH_2)_9CH_3$), 1.80 (2H, m, $-NCH_2CH_2(CH_2)_9CH_3$), 3.93 (3H, s, $-NCH_3$), 4.13 (2H, t, J = 7.40 Hz, NCH_2), 7.22 (1H, s, *H*(5)), 7.29 (1H, s, *H*(4)), 9.21 (1H, s, *H*(2)). ^{13}C NMR (75 MHz, CD_3CN): δ/ppm 13.08, 22.08, 25.37, 28.30, 28.77, 28.92, 29.03, 29.30, 31.33, 35.52, 49.22, 121.95, 123.32, 135.78.

1-Methyl-3-tetradecylimidazolium Bis(trifyl)imide, [C_{14}−mim][TFI]. Lithium bis(trifluoromethanesulfonyl)imide (6.4 g, 0.022 mol) was added to a stirred solution of 1-methyl-3-tetradecylimidazolium chloride (6.92 g, 0.022 mol) in H_2O (250 cm^3) at 70 °C. The solution was cooled to room temperature and formed a biphasic mixture. The upper, aqueous phase was decanted, and the lower phase was washed with water (100 cm^3). After it was cooled to 0 °C, the salt crystallized. It was collected by filtration, dissolved in dichloromethane (50 cm^3), and dried over $MgSO_4$, and the solvent was removed under reduced pressure and finally in vacuo at 55 °C to yield a colorless liquid which crystallized on cooling (yield 13.75 g, 100%). ^1H NMR (500 MHz, $CDCl_3$): δ/ppm 0.81 (3H, t, J = 6.51 Hz, $-N(CH_2)_{13}CH_3$), 1.18−1.25 (22H, m, $-NCH_2CH_2(CH_2)_{11}CH_3$), 1.79 (2H, m, $-NCH_2CH_2(CH_2)_9CH_3$), 3.88 (3H, s, $-NCH_3$), 5 4.09 (2H, t, J = 7.45 Hz, NCH_2), 7.19 (1H, s, *H*(5)), 7.23 (1H, s, *H*(4)), 8.70 (1H, s, *H*(2)). ^{13}C NMR (75 MHz, $CDCl_3$): δ/ppm 13.08, 22.09, 25.37, 28.30, 28.77, 28.92, 29.03, 29.06, 29.09, 29.28, 31.35, 49.26, 121.98, 123.35, 135.51.

Results

DSC Data. Table 1 shows the transition temperatures (to the nearest degree), enthalpies, and assignments from the onset temperatures of the heating cycles from the DSC. The assignments shown in the table were confirmed by the POM and SAXS data detailed below. Both the chloride and bromide salts showed thermal hysteresis when crystallized from the isotropic liquid or liquid crystalline phases, with the solidification temperature depressed by up to 30 °C. The isotropic → mesophase transition did not show significant supercooling when compared with the corresponding mesophase → crystalline phase transition.

On the first heating cycle, the hydrated chloride and bromide salts all melt ca. 30−80 °C with a large endothermic transition to a mesophase (Table 1, first heat), which clears at higher temperature with a small endothermic transition. On the first heating, the DSC showed different transitions compared with the second heating and cooling cycle. Samples were heated in open DSC pans to 250 °C and then held at this temperature for 5 min. This enabled complete in situ dehydration of the samples as shown by the change in the heat flow in the DSC thermogram. On the second and subsequent heating and cooling cycles, the transitions were reproducible, and in all cases, the transition temperatures were lower than for the initial heating scan, as shown for the second heating cycle in Table 1. This may be compared with the triflate and bis(trifyl)imide salts which show the same thermal behavior on the first and second heating scans. These effects were reproducible for any given sample.

The DSC data indicates the formation of an enantiotropic thermotropic mesophase for the triflate salts with the longest chains (n = 16, 18). The mesophase range for these salts is relatively small, 9 and 38 °C, respectively, compared with approximately 160 °C for the corresponding chloride salts. The short-chain triflate salts (n = 12, 14) and all the $[TFI]^-$ salts melt from the crystalline phase into an isotropic liquid and on cooling crystallize directly, i.e., with no mesophase observed.

As reported for the $[BF_4]^-$ salts,[15] the enthalpy of the endothermic crystal → mesophase transition (for the anhydrous salts) or crystal → isotropic transition varies with both n and the anion but, in most of the examples, is in the range of 20−50 kJ mol^{-1}. The enthalpy of the mesophase → isotropic transition in all the mesomorphic examples is small (∼1 kJ mol^{-1}).

POM Characterization. For the mesomorphic salts, X = Cl^-, $[BF_4]^-$; n = 12−18, X = Br^-; n = 12−16, 20, and X = $[OTf]^-$; n = 16 and 18, on both cooling from the isotropic liquid and heating from the crystalline solid, a single enantiotropic mesophase is observed by POM. This phase was identified initially as a thermotropic smectic A phase,[22] on the basis of the texture displayed. Samples cooled from the isotropic melt appeared black (i.e., with a uniform homeotropic texture) when they were viewed under cross polarizers, which requires that the lamellar phase be uniaxial. On deformation, samples displayed an oily streak texture, and cooling to the isotropic → mesophase transition resulted in transient focal conic domains, characteristic of a smectic A phase. This identification is supported by the SAXS data described below, with the mesophase confirmed as an interdigitated bilayer smectic A phase (denoted as SmA_2).[23]

SAXS. SAXS data was collected for the Cl^-, Br^-, $[OTf]^-$, $[TFI]^-$, and $[BF_4]^-$ salts as a function of temperature. All the salts display layered structures in both

(22) Demus, D.; Goodby, J.; Gray, G. W.; Speiss, H.-W.; Vill, V. *Handbook of Liquid Crystals, High Molecular Weight Liquid Crystals*; Wiley-VCH: New York, 1998; Vol. 3.

(23) Gray, G. W.; Goodby, J. *Smectic Liquid Crystals, Texture and Structure*; Leonard Hill: Glasgow, 1984.

Table 2. Layer Spacing (*d*, Å) Determined in the Crystalline Phase and in the SmA_2 Phase at 80 °C Based on the Position of the Lowest-Angle Diffraction Peak in the SAXS Data on Cooling

		layer spacing (*d*), Å	
n	anion, X^-	crystal	SmA_2
12	[TFI]	24.7	
14		25.2	
16		28.2	
18		28.8	
12	[OTf]	26.8	
14		29.4	
16		28.2/36.0	31.6
18		30.3/43.4	34.4
12	$[BF_4]$		
14		27.2	31.4
15		28.6	33.0
16		32.1	35.4
18		34.6	37.7
12	Br	22.8	32.0
14		27.0 (53.5[a])	33.6
16		30.7	36.3
20		31.6	38.8
12	Cl	22.5	31.7
14		25.8 (50.7[a])	34.4
16		29.0 (56.6[a])	36.7
18		31.0 (60.9[a])	41.2

[a] Peak due to double/extended bilayer spacing found on initial heating.

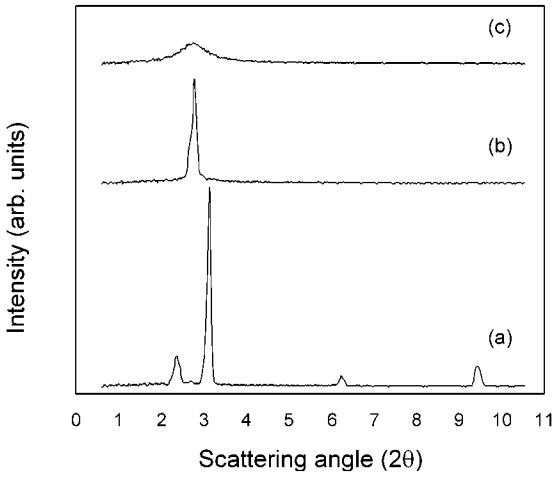

Figure 2. SAXS pattern for $[C_{16}-mim][OTf]$ at (a) 50 °C, (b) 70 °C, and (c) 90 °C in the crystal, SmA_2, and isotropic phases, respectively, on cooling.

the crystal and liquid crystalline phases, with one or more peaks in the low-angle region of the diffraction pattern. The layer spacing (*d*) was calculated by using Bragg's law. The samples studied and layer spacings, determined from the lowest-angle feature, in the crystal and liquid crystalline phases on cooling from the isotropic liquid are given in Table 2. Typical SAXS data collected for $[C_{16}-mim][OTf]$ in the crystal, liquid crystal, and isotropic liquid regions is shown in Figure 2.

In the mesophase, all the salts display a similar, characteristic SAXS pattern, consisting of at least one narrow peak in the low-angle region ($2\theta = 1-5°$), which corresponds to a layer spacing (*d*) between 22 and 61 Å (see Table 2). For each anion, the layer spacing of the mesophase increases monotonically with the alkyl-chain length, *n*, and decreases with increasing temperature

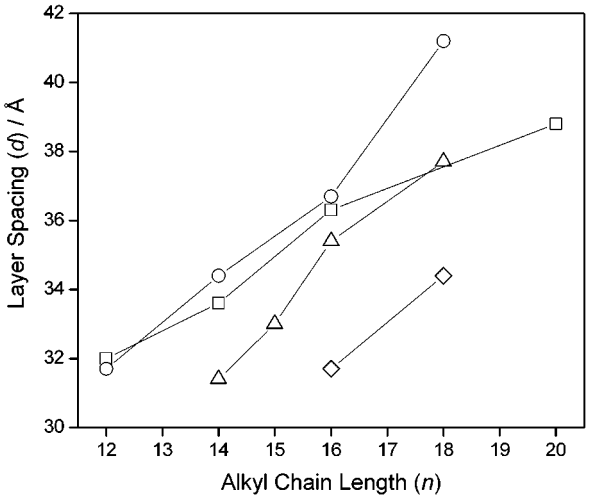

Figure 3. Dependence of the SmA_2 layer spacings of the chloride (○), bromide (□), tetrafluoroborate (△), and triflate (◇) salts on *n* at 80 °C.

as shown in Figures 3 and 4, respectively. The temperature variation reflects the greater thermal mobility of the alkyl chains, i.e., increased melting of the alkyl phase. The layer spacing in the mesophase, for a given cation, depends on the anion present and decreases following the order $Cl^- > Br^- > [BF_4]^- > [OTf]^-$.

The SAXS data collected from the crystalline phase show that there are up to two different phase types that are formed, depending on the thermal history of the sample, i.e., whether dehydration had occurred. The most intense peak in the low-angle region corresponds to the (001) layer repeat unit. For each of the anions studied, the layer spacing in the crystal is *smaller* than the layer spacing in the mesophase. For example, in Figure 2, the (001) layer spacing is 28.2 Å whereas in the mesophase, a single, intense peak is found corresponding to a layer spacing of 31.6 Å. The same observation has been made from reflectivity studies on $[C_{18}-mim][BF_4]$ deposited as a thin film on Si(111).[9]

Since the crystal layer spacing is $l < d < 2l$, where *l* is the fully extended alkyl-chain length, this indicates that in the crystal structure, the alkyl chains of the cations are interdigitated and/or tilted with respect to the layer normal. The layer spacing increased on transforming from the crystal to the mesophase, which indicates that the structure undergoes a conformational change in addition to alkyl-chain melting, for example, decreasing the angle of tilt with respect to the layer normal.

In Figure 2, the other peaks observed in the low-angle region for the crystalline phase, for example, the peak at 2.45° corresponding to a spacing of 36.0 Å, are much less intense and do not fit the regular repeat unit of the layer structure (determined from the (001) and (002) peaks at $2\theta = 3.15$ and 6.30°). This particular feature is possibly due to a different layer spacing arising from conformational disorder of the cation. For example, both bent and linear alkyl-group geometries relative to the ring position have been observed in the crystal structures of 1-alkyl-3-methylimidazolium salts.[24]

Peaks are also found in the wide-angle data for the crystalline phase. For example, in $[C_{16}-mim][OTf]$, a peak corresponding to 9.4 Å is observed. This corre-

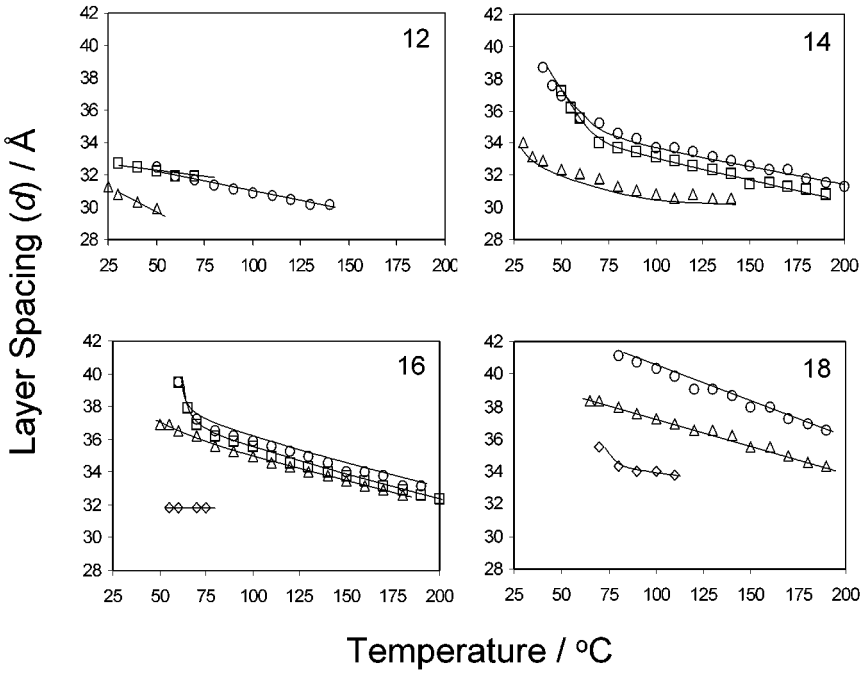

Figure 4. Dependence of the SmA_2 layer spacing (d) on temperature for the [C_n−mim]X salts (n = 12−18): X = chloride (○), bromide (□), tetrafluoroborate (△), and triflate (◊).

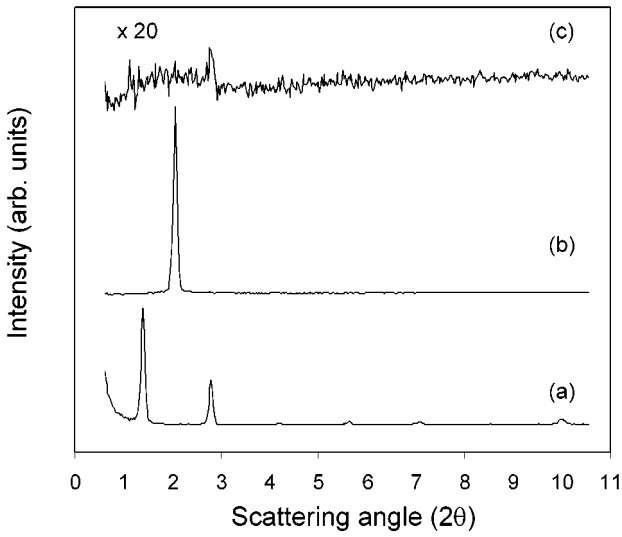

Figure 5. SAXS pattern for [C_{18}−mim]Cl at (a) 30 °C, (b) 75 °C, and (c) cooled back to 30 °C, i.e., in the crystal, SmA_2, and back to the crystalline phase, respectively.

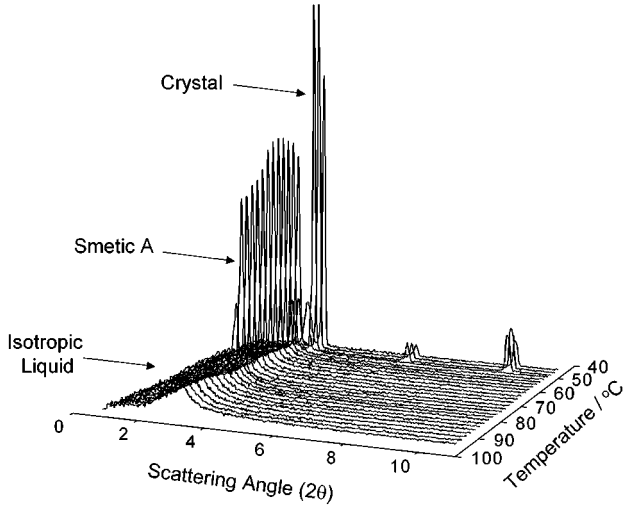

Figure 6. Development of the SmA_2 and crystalline phases from molten, isotropic [C_{16}−mim][OTf] on cooling.

sponds to the cation−cation and anion−anion repeat distance within the layers.[24]

In some examples (particularly, the chlorides and bromides), a peak is also found at low angles (approximately 1−2°). Figure 5 shows the heating and cooling cycle for [C_{18}−mim]Cl. The peaks at 1.44 and 2.89° are consistent with a d spacing of 60.9 Å corresponding to the (001) and (002) reflections, respectively, in the monohydrate structure. After cooling from the isotropic liquid, i.e., after dehydration to the anhydrous salt, only one peak is observed at 2.84° corresponding to the (001) peak associated with a d spacing of 31.0 Å. The large periodicity of the hydrated crystalline phase, prior to melting and dehydration, may be explained in two ways: either a double bilayer structure or extended bilayer in which the alkyl chains are not interdigitated but are packed from end to end. It should be noted that there is a significant decrease in the signal-to-noise on cooling. This indicates that the liquid crystal undergoes a glass transition and although some order is present it is much reduced on thermal crystallization compared with solvent crystallization.

In the mesophase, the peak in the wide-angle region, observed in the crystalline phase, is lost which indicates a decrease in positional ordering within the layer plane. In the isotropic liquid phase, above the melting point, a broad low intensity scattering peak was observed. Figure 6 shows the time-resolved SAXS data obtained

(24) (a) Holbrey, J. D.; Nieuwenhuyzen, M.; McCormac, P.; Johnston, S.; Seddon, K. R. Unpublished results. (b) Downard, A.; Earle, M.; Nieuwenhuyzen, M.; Seddon, K. R., submitted to *J. Chem. Soc., Chem. Commun.*

for $[C_{16}-mim][OTf]$ on the first cooling cycle (ramp rate = 6 °C min^{-1}, data collected in 12 s frames) from the isotropic melt. The broad peak in the isotropic region, the single sharp peak in the SmA_2 mesophase, the higher-order peaks in the crystalline phase, and the phase transitions, isotropic → SmA_2 and SmA_2 → crystal, are clearly visible at 72 and 61 °C, which correlates well with the DSC data.

For the bis(trifyl)imide salts, which do not exhibit a liquid crystalline phase, data were collected in the crystalline and isotropic phases. The crystalline phases of the salts ($n = 14-18$) show a SAXS pattern consistent with a layered structure, and as with the other anions studied, the layer spacing increases with n. When melted to the isotropic phase, a broad peak is observed in the SAXS data for each salt, as shown by the other anions. This peak indicates that for all the salts studied, the isotropic liquid phase still retains some short-range associative structural ordering.

Discussion

All of the salts that were studied melt between 15−75 °C. The temperature of the melting point transition (cryst → iso or cryst → SmA_2) varies only slightly with n, increasing by approximately 10 °C for each ethylene unit added to the alkyl chain. In contrast, the clearing point (in the mesomorphic examples) increases more rapidly with n, i.e., the temperature range of the SmA_2 phase increases with increasing alkyl-chain length. Crystal−crystal polymorphism was not observed for any of the salts over the temperature range of 25−250 °C. This is in contrast to the long-chain 1-alkyl-3-methylimidazolium tetrachloropalladate(II) salts,[16] which showed extensive crystal−crystal polymorphism. The potential for polymorphism in the subambient temperature regime was not investigated in this study.

The detailed analysis of the thermal behavior of the chloride and bromide salts shows that data initially communicated for the $[C_n-mim]Cl$ series ($n = 12-18$)[12] was, in fact, for hydrated rather than the anhydrous chloride salts. This can be attributed to the hygroscopic nature of the halide salts and reflects the difficulties encountered in maintaining truly anhydrous salts under laboratory conditions. The lower transition temperatures (and the melting enthalpy) of the anhydrous chloride and bromide salts compared with their respective hydrates indicates that there is significant structural stabilization derived from hydrogen-bonding with water in these systems. This has been observed previously for the salts 1,3-dimethylimidazolium chloride hemihydrate and 1-ethyl-3-methylimidazolium chloride hydrate. In each case, an extended hydrogen-bonded lattice of water and chloride ions has been identified in the single-crystal X-ray structure.[25] The water can be removed by heating under vacuum; however, it should be noted that on extended heating at elevated temperatures, there is a significant risk of thermal degradation of the samples.[26]

The SAXS data provides an insight into the relationship between the structure and liquid crystalline properties of the salts and by extension into the relationship between the structure and solvating properties of the wide range of analogous ionic liquids. The melting transition (to mesophase or isotropic liquid) in each case is similar and is caused primarily by alkyl-chain melting. In those salts which exhibit a mesophase, the structural motif is maintained on forming the liquid crystal by attractive van der Waals forces within the ionic plane.[27] This is also present to some degree on melting to the isotropic liquid phase and indicates that the structures found in the crystal and liquid crystalline regions may be used qualitatively to describe that in the liquid. In this study, it could be argued that the ordering in the liquid is simply a consequence of the long alkyl chains. However, similar results have also been noted for dimethyl imidazolium chloride using neutron scattering.[28]

The chloride, bromide, and tetrafluoroborate salts display a mesophase with a thermal range that is >90 °C in general, whereas in the case of $[TFI]^-$ and $[OTf]^-$, only a small mesophase range ($[OTf]^-$, $n = 16, 18$) or no mesomorphism ($[TFI]^-$) is observed. The ability to stabilize a mesophase appears to follow the ability of the anion to form a three-dimensional hydrogen-bonding lattice, i.e., $Cl^- > Br^- > [BF_4]^- > [OTf]^- > [TFI]^-$. For example, although $[BF_4]^-$ has a smaller tendency to form hydrogen bonds than $[OTf]^-$, the anion is spherical and therefore can form bonds in all directions. Thus, there is a greater possibility of the anion directing the cation structure within the charged region resulting in a larger interlayer spacing than that for $[OTf]^-$. The structure in the liquid crystalline phase is determined by the anion−cation interactions within the polar region. This order is observed, to a lesser degree, in the liquid structure, and therefore, it is likely that the anion dependence observed for these salts will also be present in the liquid structure of shorter-chain ionic liquid analogues.

The mesomorphic examples (containing chloride, bromide, tetrafluoroborate, and triflate anions) melt from the crystalline phase to an enantiotropic smectic A mesophase. The layer spacing in the mesophase, determined from the SAXS data, for each of the salts is consistent with a SmA_2 phase, where the alkyl chains may remain interdigitated as in the crystalline phase but are disordered. The melting transition produced an increase in the layer spacing of the salts, compared with the crystalline phases, based on the position of the highest intensity peak in the SAXS diffractograms. The crystalline phases then are most likely to be biaxial and interdigitated, with alkyl chains tilted with respect to the bilayer normal.

The halide salts appear to adopt one of two distinct conformational lattices which are characterized by a bilayer or an extended/double bilayer repeat unit based on the d spacing from the lowest-angle peak in the diffractogram. The bromide salts $[C_n-mim]Br$ ($n = 12$, 16, 20) and $[C_{12}-mim]Cl$ have layer spacings consistent with a normal bilayer structure ($d < 2l$). In contrast, $[C_n-mim]Cl$ ($n = 14, 16, 18$) and $[C_{14}-mim]Br$ display the two peaks in the low-angle region as in Figure 5.

(25) Elaiwi, A. E. Mass spectrometry of organic and chlorometalated salts. Ph.D. Thesis, University of Sussex, U.K., 1994.
(26) Chan, B. K. M.; Chang, N.-H.; Grimmett, M. R. *Aust. J. Chem.* **1977**, *30*, 2005.
(27) Paleos, C. M. *Mol. Cryst. Liq. Cryst.* **1994**, *243*, 159.
(28) Bowron, D. T.; Hardacre, C.; Holbrey, J. D.; McMath, S. E. J.; Soper, A. K. Unpublished results.

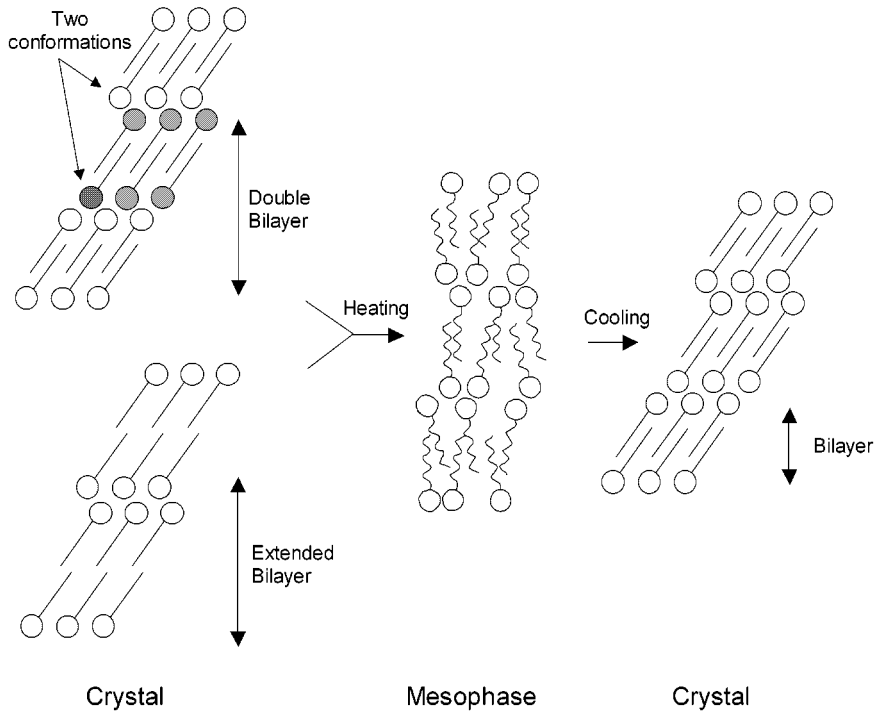

Figure 7. Schematic of the melting of the double and extended bilayer structures in the crystalline phase of, for example, $[C_{18}$–mim]Cl to the mesophase and subsequent recrystallization from the melt.

These peaks correspond to a repeat unit of approximately twice the molecular length (l) of the fully extended cation, e.g., for $n = 18$, $d = 60.9$ Å and $l = 31$ Å, based on molecular models.

This large layer spacing may be explained by two models shown schematically in Figure 7. The double bilayer model relies on differing conformations of the headgroups in alternating layers. Crystal packing allows the two conformers to be present in the hydrated form, whereas following dehydration to the anhydrous salt and cooling, only the most stable form is crystallized resulting in the one conformer. Similar structures are known, for example, two different cation conformations are observed in the crystal structure of the related hexadecylpyridinium bis(3,6-dichloro-4,5-dioxo-2,6-cyclohexadiene-1,2-dionato)-beryllium salt.[29] The extended bilayer model simply refers to a lamellar, bilayer structure with no alkyl-chain interdigitation, i.e., end to end packing of the alkyl chains. Although it is not possible to distinguish the two scenarios using the data presented here, it is more likely that the interdigitated structure is formed. Single-crystal X-ray diffraction would be able to elucidate the structure; however, to date, we have been unable to obtain crystals of these salts of a quality sufficient for a full structure determination due to the formation of very thin platelike crystals.

(29) Burzlaff, H.; Lange, J.; Spengler, R.; Karayannis, M. I.; Veltsistas, P. G. *Acta Crystallogr., Sect. C* **1995**, *51*, 190.

Conclusions

The thermal behavior of long-chain 1-alkyl-3-methylimidazolium salts with a range of anions of differing coordinating ability and size from chloride to bis(trifluoromethanesulfonyl)imide have been studied by DSC, POM, and SAXS. The salts, with $X = Cl^-$, Br^-, $[BF_4]^-$, and $[OTf]^-$ ($n = 16$, 18), display a thermotropic liquid crystalline mesophase. The shorter-chain triflate salts ($n = 12$, 14) and the bis(trifluoromethanesulfonyl)imide salts melt, with no mesomorphism, to form isotropic liquids. The layer spacing in the crystal and mesophase has been determined from variable temperature SAXS and indicates that the layer spacing in each phase varies with both n and the anion present. The layer spacing increases with n and with the coordinating ability of the anion present, following the anion order $Cl^- > Br^- > [BF_4]^- > [OTf]^- > [TFI]^-$. This represents a measure of the ability of the anions to hydrogen-bond and build *extended* structures within the ionic region of the layered phases.

Acknowledgment. The authors would like to thank Unilever (A.E.B.), DENI and QUILL (S.E.J.McM) for financial support, and the EPSRC for SAXS beamtime (Grant No. GR/M89775).

Supporting Information Available: Table containing analytical data for the salts synthesized (PDF). This material is available free of charge via the Internet at http://pubs.acs.org.

CM010542V